Waveguide-type optical circuits for recognition of optical 8PSK-coded labels

Munkhbayar Adiya[1], Nyam-Erdene Odbayar[1 *], Hiroki Kishikawa[1 †], Nobuo Goto[1], Ganbold Shagdar[2]

[1]*Department of Optical Science, Tokushima University, 2-1 Minamijosanjima-cho, Tokushima, 770-8506 Japan*

[2]*Mongolian University of Science and Technology, School of Information and Communication Technology, Ulaanbaatar-13343, Mongolia*

This paper discusses optical label recognition for photonic label routing. The label recognition is one of the key function in photonic label routing related functions including optical label extraction, recognition of the label and label rewriting. In previous study, we have proposed a basic waveguide-type circuit for recognition of optical label encoded in quadri-phase-shift-keying (QPSK) format, which consists of 3-dB directional coupler, two Y-branches and an asymmetric X junction coupler. In order to increase the number of labels represented by the same symbol number, we propose 8PSK recognition circuits based on the QPSK recognition circuit. The input-output relation of the proposed circuits is theoretically discussed and the noise tolerance is also investigated. From the theoretical analysis, the proposed optical-waveguide circuits recognize the 8PSK labels by detecting the position of the output port having either the maximum or minimum intensity. The bit-error performance of the proposed circuits is clarified by computer simulation. It is found that the minimum-output detection scheme for one-symbol 8PSK label is superior from the viewpoint of noise tolerance. The proposed method also addresses the scalability of two-symbol 8PSK coded labels. The maximum-output detection scheme demonstrates improved scalability performance.

1. Introduction

Technological development in telecommunication systems to meet the growing demand of communication traffic requires faster speed, larger capacity and broader-band transmission. In conventional optical network systems, electrical signal processing is applied to the routing node together with optical-to-electrical and electrical-to-optical conversion. This conversion takes time for processing and requires power consumption which makes transmission system more complex. The optical signal processing without conversion to electrical signals is expected to be applied to routing nodes to overcome those disadvantages.[1)]

*M. Adiya and N. Odbayar equally contributed to this work.
†E-mail: kishikawa.hiroki@tokushima-u.ac.jp

Various optical signal processing functions performed in routers include optical label extraction, recognition of the label, optical switching and buffering, and label rewriting. We focus on photonic label recognition methods among these signal processing functions. As one of the nature of light, phase of coherent light has been effectively used in various optical systems, where the passive interference behavior between multiple signals is easily used. Using this feature, label recognition techniques have been investigated for photonic routers based on optical code correlation.[2–9] However, most of the proposed systems could not recognize all the binary codes because only the type of codes that provide enough discrimination between auto-correlation and cross-correlation were recognized.[4,10–12] A self-routing architecture was proposed for the label recognition system in which optical active elements have chosen to identify label information,[13] where multiple label recognition for on-off keying (OOK) codes was achieved. Other types of optical label recognition techniques include an optical method based on optical serial-to-parallel conversion and spin-polarized all-optical switch,[14] a method using optical digital-to-analog conversion,[15] and a CMOS-based low-power-consumption label processor.[16] On the other hand, an all-optical passive label recognition system for all the binary codes in binary phase-shift-keying (BPSK) format was proposed.[17] This passive processing scheme provides faster and power efficient processing.[18] Even though, self-routing architecture for label recognition is one of the promising methods in label decoding system, the number of data streams in transmission systems is enormous, which requires a large number of routing labels in the networks. The number of represented labels increases by employing multiple phases such as quadri-phase-shift keying (QPSK) and quadrature amplitude modulation (QAM) coded labels.[19–22)]

The QAM modulated pulses have multiple amplitudes, which results in efficient bandwidth and high bit rate for transmission. Although the distance between each of the QAM codes in the signal constellation may be larger compared with a single amplitude codes such as multiple PSK codes, optical recognition scheme for such M-ary PSK labels is much simpler. Therefore, we propose optical recognition circuits for 8PSK coded labels. The proposed circuit is based on the optical QPSK recognition circuit (QPRC)[23] which consists of an asymmetric X-junction coupler, Y-branches and a 3-dB directional coupler. We have proposed two recognition schemes, that are recognition from maximum output port or from minimum output port. The recognition characteristics for one-symbol labels by maximum-output scheme was reported.[24] For minimum-output scheme, we reported for one- and two-symbol labels.[25] In this paper, we compare these two schemes for one- and two-symbol labels from the view point of noise tolerance. The electrical power consumption of the proposed circuit is consid-

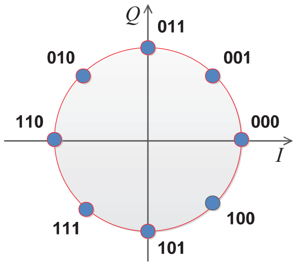

Fig. 1. Constellation of 8PSK coded signals.

ered to be low because of the passive integrated-optic devices and thresholders. The recognition is performed during optical wave propagation through the proposed passive devices and thresholders. Therefore, the processing speed is expected to be fast.

The proposed waveguide-type 8PSK recognition circuit employs two decision schemes, i.e., recognition from the maximum output port or from the minimum output port. First, the input-output relation of the recognition circuit is theoretically analyzed. Then, the bit-error-rate (BER) characteristics against optical signal-to-noise ratio (OSNR) are evaluated by numerical simulations using OptiSystem software (Optiwave Systems Inc.) in order to clarify the label recognition performance since noise tolerance is considered as one of the important factors in the telecommunication system. For the purpose of comparison, we also build a back-to-back (B2B) model which uses a digital coherent receiver to recognize 8PSK codes.

In the optical label network system, a large number of routing labels are required. It is reported that thousands to tens of thousands of labels are required.[4)] Thus, we propose scaled two-symbol-length 8PSK label recognition circuits for the two recognition schemes. Similar scaled circuits can be configured for more than three-symbol-length labels. We evaluate and compare the BER characteristics between the two recognition schemes.

This paper consists of 4 sections. In Section 2, we describe the proposed recognition circuits and their theoretical analysis. The noise tolerance of the recognition performance is numerically simulated in Section 3. Finally, the conclusions are presented in Section 4.

2. 8PSK-Coded Label Recognition Circuit

The constellation diagram of 8PSK codes is illustrated in Fig. 1. The types of PSK include BPSK, QPSK, and M-ary PSK (8PSK, 16PSK, $\cdots$). In the 8PSK codes, the carrier phase is shifted by 8 times and each phase represents 3 bits information.

An example of the optical processing for label recognition is schematically illustrated in Fig. 2. We assume that an extracted optical label from an incident packet to the router

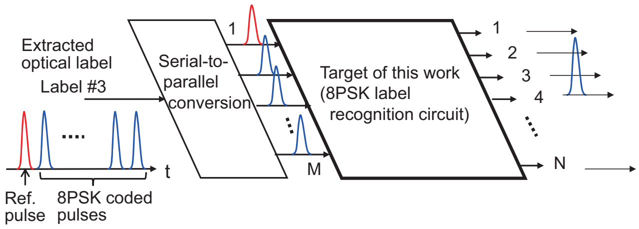

Fig. 2. Optical processing with a label recognition circuit.

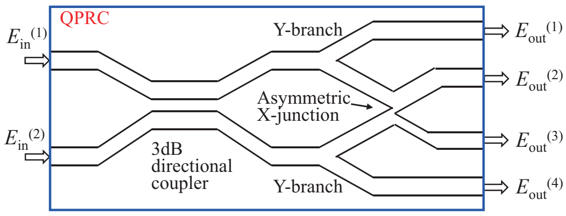

Fig. 3. Basic integrated-optic circuit module for recognition of QPSK coded labels.

is a time-series pulse train including a reference pulse. The reference pulse plays a role to identify the phase of the labels. After the preprocessing with serial-to-parallel converter,[17] the parallel pulses are incident into the label recognition circuit. The number of output ports N is assumed to be equal to the number of labels to be recognized. The incident label is identified as the output port number having the maximum or minimum optical intensity. The serial-to-parallel conversion might not be necessary when time gates or appropriate thresholding devices are employed at the output ports in post-processing.[19] In this paper, we focus on the label recognition circuit after serial-to-parallel conversion for simplicity.

2.1 One-symbol 8PSK label recognition

The basic optical waveguide circuit module, QPRC, proposed for recognition of QPSK labels is shown in Fig. 3. This circuit consists of a 3-dB directional coupler, two Y-branches and an asymmetric X-junction coupler. The combination of the transmission characteristics of these basic components with a reference signal in one of the inputs is used to recognize the phase of incident QPSK signals. In this circuit, we have 2-input and 4-output signals. The input and output relation can be written as:[19,26]

$$\begin{pmatrix} E_{\text{out}}^{(1)} \\ E_{\text{out}}^{(2)} \\ E_{\text{out}}^{(3)} \\ E_{\text{out}}^{(4)} \end{pmatrix} = A_{\text{QPRC}} \begin{pmatrix} E_{\text{in}}^{(1)} \\ E_{\text{in}}^{(2)} \end{pmatrix}, \tag{1}$$

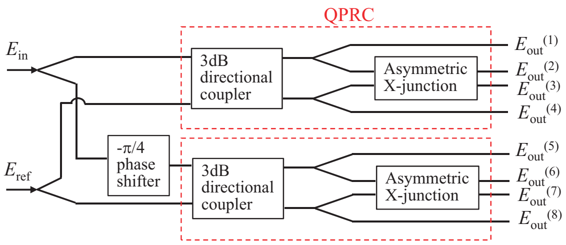

Fig. 4. Proposed integrated-optic circuit for recognition of 8PSK coded labels.

where

$$A_{\mathrm{QPRC}} = \frac{1}{2}\begin{pmatrix} 1 & e^{j3\pi/2} \\ e^{j7\pi/4} & e^{j7\pi/4} \\ e^{j5\pi/4} & e^{j\pi/4} \\ e^{j3\pi 2} & 1 \end{pmatrix}. \tag{2}$$

From these equations, it is found that each QPSK signal at $E_{\mathrm{in}}^{(1)}$ with a reference pulse at $E_{\mathrm{in}}^{(2)}$ produces the maximum and null output optical intensity at a different output port corresponding to the phase of the incident signal. This function is similar to an optical 90° hybrid module.[27,28)]

Our proposed 8PSK recognition circuit (8PRC) consists of two QPRCs, two Y-branches, and a phase shifter as shown in Fig. 4. A $-\pi/4$-phase shifter is introduced to identify all of the phase values of given 8PSK coded signals. The 8PSK recognition circuit has 2-inputs and 8-output ports. We consider an input 8PSK signal as E_{in} given by

$$E_{\mathrm{in}} = E_0 e^{jn\pi/4}, \quad (n = 0, 1, \ldots, 7), \tag{3}$$

and a reference signal E_{ref} as given by

$$E_{\mathrm{ref}} = E_0. \tag{4}$$

The output optical fields from the recognition circuit are related to the input signals as:

$$\begin{pmatrix} E_{\rm out}^{(1)} \\ \vdots \\ E_{\rm out}^{(8)} \end{pmatrix} = A_{\rm 8PRC} \begin{pmatrix} E_{\rm out}^{(1)} \\ \vdots \\ E_{\rm out}^{(8)} \end{pmatrix} = \begin{pmatrix} A_{\rm QPRC} & 0 \\ 0 & A_{\rm QPRC} \end{pmatrix} \begin{pmatrix} \frac{1}{\sqrt{2}} & 0 \\ 0 & \frac{1}{\sqrt{2}} \\ \frac{e^{-j\pi/4}}{\sqrt{2}} & 0 \\ 0 & \frac{1}{\sqrt{2}} \end{pmatrix} \begin{pmatrix} E_{\rm in} \\ E_{\rm ref} \end{pmatrix}$$

$$= \frac{E_0}{2\sqrt{2}} \begin{pmatrix} e^{j\pi n/4} + e^{j3\pi/2} \\ e^{j(7+n)\pi/4} + e^{j7\pi/4} \\ e^{j(5+n)\pi/4} + e^{j\pi/4} \\ e^{j(6+n)\pi/4} + 1 \\ e^{j(n-1)\pi/4} + e^{j3\pi/2} \\ e^{j(6+n)\pi/4} + e^{j7\pi/4} \\ e^{j(4+n)\pi/4} + e^{j\pi/4} \\ e^{j(5+n)\pi/4} + 1 \end{pmatrix}. \tag{5}$$

As a result of this equation, there are five different optical intensities at each of the output ports. Fig. 5 shows the theoretical relative output intensities $|E_{\rm out}^{(k)}/E_0|^2$ for eight codes. It is found that one output port has the maximum intensity for each 8PSK code. In addition, one output port has the minimum (null) intensity for each 8PSK code. The maximum and the minimum intensities are 0.5 and 0, respectively. The second maximum intensity of 0.427 (85.4 % of the maximum intensity) appears at two output ports. The second minimum intensity of 0.073 (14.6 % of the maximum intensity) appears also at two output ports. Two recognition schemes are considered according to this theoretical calculation, i.e., maximum or minimum output port is used for the code recognition. A threshold processing is performed at the intensity between the maximum and the second maximum intensities to identify the phase of the 8PSK coded labels in the maximum-output scheme. Similarly, the threshold processing is performed at the intensity between the minimum and the second minimum intensities in the minimum-output scheme.

2.2 Two-symbol 8PSK label recognition

We consider two-symbol 8PSK recognition circuits to study the scalability of the proposed recognition circuits. The circuit structures of the maximum-output and the minimum-output detection schemes are different.

2.2.1 Maximum-output detection scheme Figure 6 shows a two-symbol recognition circuit by the maximum-output detection scheme. The circuit has a two-stage connection of the 8PRCs. The first symbol pulse and the reference pulse are incident into 8PRC 1-1. The

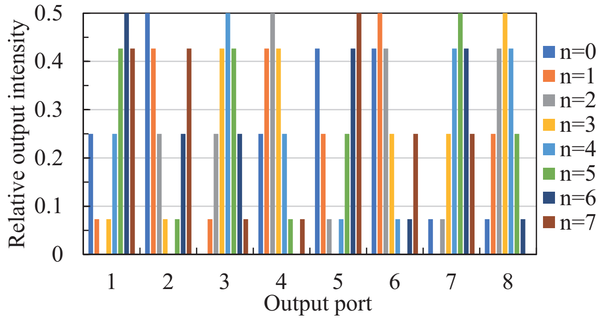

Fig. 5. Theoretical output intensities for 8PSK codes.

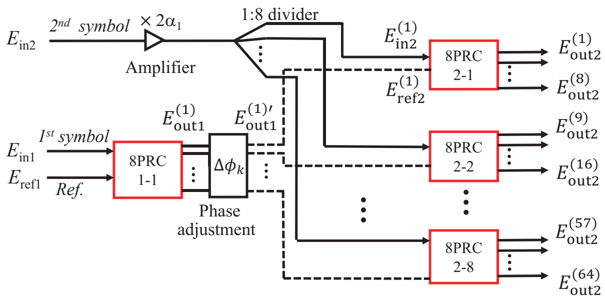

Fig. 6. Optical circuit for 2 symbol 8PSK label recognition by maximum-output detection scheme.

output signals from 8PRC 1-1 are sent to the second stage 8PRCs as the reference signals $E^{(k)}_{\mathrm{ref2}}$, $k = 1, \ldots, 8$, after the phase adjustment ϕ_k. The second symbol pulse is amplified with an amplitude amplification coefficient of $2\alpha_1$, and divided into 8 signals to the second stage 8PRCs as $E^{(k)}_{\mathrm{in2}}$.

The output signals from the first stage 8PRC are used as the reference signal in the second stage 8PRCs. The phase of the maximum output signal differs depending on the maximum output port. Therefore, the maximum output signal from the first stage 8PRC is required to adjust in phase to make a complete interference between the reference signal and the second symbol signal. The output fields $E^{(k)\prime}_{\mathrm{out1}}$, $(k = 1, \ldots, 8)$ are phase shifted by ϕ_k from the input fields $E^{(k)}_{\mathrm{out1}}$, where the phase shift amounts are set to be $\phi_1 = \phi_5 = \pi/2$, $\phi_2 = \phi_6 = \pi/4$, $\phi_3 = \phi_7 = -\pi/4$, and $\phi_4 = \phi_8 = 0$. The outputs after the phase adjustment can be calculated

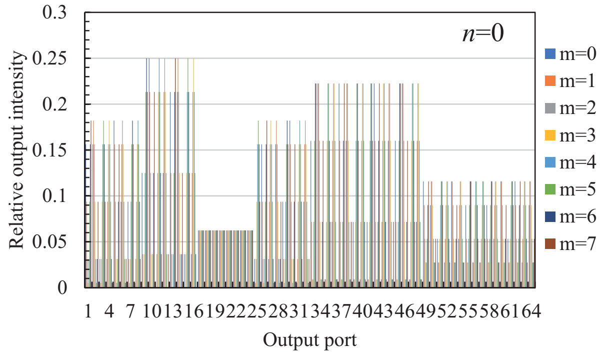

Fig. 7. Relative output intensities for two-symbol 8PSK labels by maximum-output scheme.

by eq.(5) and the phase shift amount ϕ_k as

$$\begin{pmatrix} E^{(1)\prime}_{\text{out1}} \\ E^{(2)\prime}_{\text{out1}} \\ E^{(3)\prime}_{\text{out1}} \\ E^{(4)\prime}_{\text{out1}} \\ E^{(5)\prime}_{\text{out1}} \\ E^{(6)\prime}_{\text{out1}} \\ E^{(7)\prime}_{\text{out1}} \\ E^{(8)\prime}_{\text{out1}} \end{pmatrix} = \frac{E_0}{2\sqrt{2}} \begin{pmatrix} e^{j(n+2)\pi/4}+1 \\ e^{j(n+8)\pi/4}+1 \\ e^{j(n+4)\pi/4}+1 \\ e^{j(n+6)\pi/4}+1 \\ e^{j(n+1)\pi/4}+1 \\ e^{j(n+7)\pi/4}+1 \\ e^{j(n+3)\pi/4}+1 \\ e^{j(n+5)\pi/4}+1 \end{pmatrix}. \tag{6}$$

The second symbol to the recognition circuit is assumed to be given by

$$E_{\text{in2}} = E_0 e^{jm\pi/4}, (m = 0, 1, \dots, 7). \tag{7}$$

The outputs from the second-stage 8PRC 2-k are calculated as:

$$\begin{pmatrix} E^{(8(k-1)+1)}_{\text{out2}} \\ \vdots \\ E^{(8(k-1)+8)}_{\text{out2}} \end{pmatrix} = A_{\text{8PRC}} \begin{pmatrix} \frac{2\alpha_1 E_0}{2\sqrt{2}} e^{jm\pi/4} \\ E^{(1)\prime}_{\text{out k}} \end{pmatrix}, \tag{8}$$

where $k = 1, \dots, 8$, and A_{8PRC} is defined in eq.(5).

Fig. 7 shows the relative output intensities $|E^{(i)}_{\text{out2}}/E_0|^2, (i = 1, \dots, 64)$ from the theoretical calculation for the case $n = 0$. Here, we set the amplitude coefficient for the amplifier as $\alpha_1 = 1$ to increase the ratio of the maximum output to the second maximum output. The maximum intensity is found to be 0.250 at the output port, port number of 10, 14, 12, 16, 11, 15, 9, 13, out of 64 ports for each input of $m = 0, 1, 2, 3, 4, 5, 6, 7$, respectively. The second maximum intensity is 0.2225 (89.0 % of the maximum intensity). Similarly, for all the combination of m and n, only one maximum output is obtained at a different port. Thus,

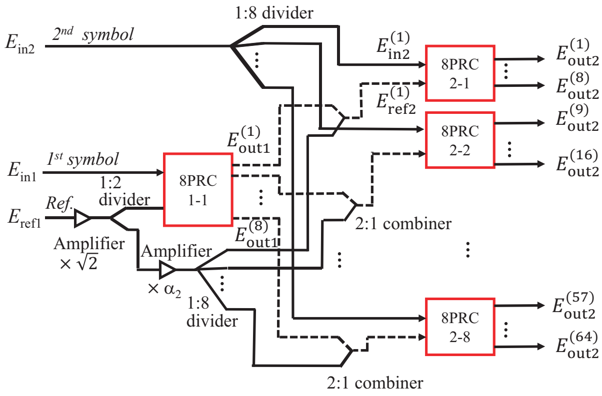

Fig. 8. Optical circuit for 2 symbol 8PSK label recognition by minimum-output detection scheme.

the two-symbol 8PSK labels can be recognized by the maximum-output scheme with our proposed recognition circuit using thresholding between 0.250 and 0.2225.

2.2.2 Minimum-output detection scheme Figure 8 shows a two-symbol recognition circuit by the minimum-output detection scheme. The circuit has a two-stage connection of the 8PRCs. The first symbol pulse $E_{\rm in1}$ is incident into the first stage 8PRC, 8PRC 1-1. The reference pulse is amplified with an amplitude amplification coefficient of $\sqrt{2}$ and divided into two pulses. The reference signal amplitude at the input port of 8PRC 1-1 is the same as $E_{\rm ref}$. The divided reference signal is amplified with an amplitude coefficient of α_2, and divided into eight signals. These divided eight signals are added to the outputs of 8PRC 1-1, and sent to the second-stage 8PRCs as the reference signals. The second symbol pulse is divided into eight signals to the second-stage 8PRCs as $E^{(k)}_{\rm in2}$.

The outputs from the second-stage 8PRC 2-k are calculated as follows by using eqs.(4) and (7):

$$\begin{pmatrix} E^{(8(k-1)+1)}_{\rm out2} \\ \vdots \\ E^{(8(k-1)+8)}_{\rm out2} \end{pmatrix} = A_{\rm 8PRC} \begin{pmatrix} \frac{E_0}{2\sqrt{2}} e^{jm\pi/4} \\ E^{(1)}_{\rm out\ k} + \frac{\alpha_2 E_0}{2\sqrt{2}} \end{pmatrix}. \tag{9}$$

It is noted that the phase adjustment circuit is not employed after 8PRC 1-1 since the null output from 8PRC 1-1 is used for a part of the reference signal to the second-stage 8PRCs. The amplification coefficient α_2 is found to be set as $\alpha_2 = \sqrt{2}$ for the complete interference.

Fig. 9(a) shows the relative output intensities $|E^{(i)}_{\rm out2}/E_0|^2, (i = 1, \ldots, 64)$ from the theoretical calculation for the case $n = 0$. The maximum output intensity is 0.160. Null outputs are obtained at ports from 17 to 24 as shown in (b). The second minimum outputs appear at ports from 49 to 56 and the intensity is 0.000785 (0.49 % of the maximum intensity).

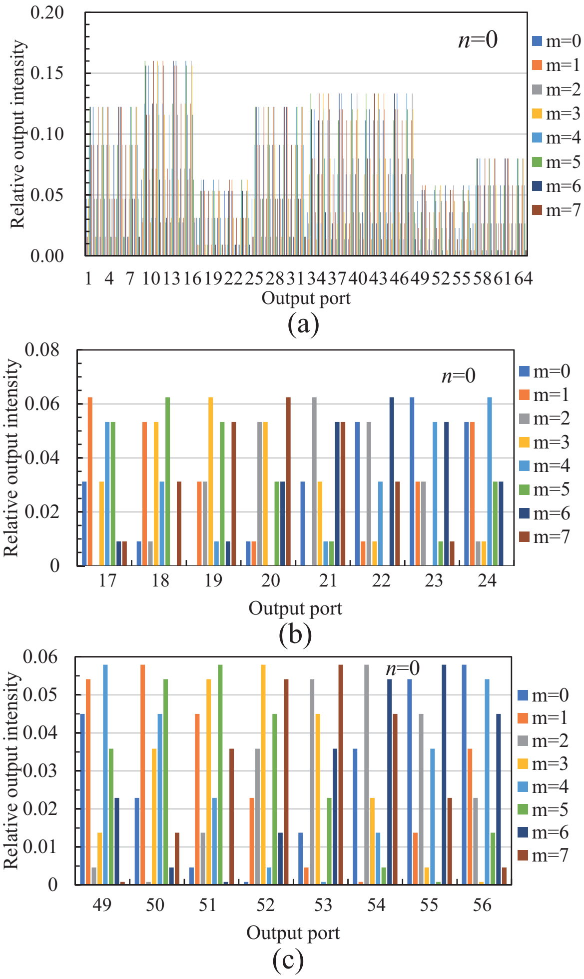

Fig. 9. Relative output intensities for two-symbol 8PSK labels by minimum-output detection for (a) output port 1 to 64, (b) output port 17 to 24, and (c) output port 49 to 56.

This small second-minimum output is caused by the phase difference between the second minimum output $E^{(k)}_{\mathrm{out1}}$ and the reference signal at the 2:1 combiners. This phase difference cannot be compensated by a phase adjustment at the output of 8PRC 1-1 because there are two phase-different second-minimum outputs for each 8PSK signal. If a phase adjustment is employed for $n = 0$, the phase adjustment cannot adjust the phase for the other n. Therefore, scalability for the minimum-output detection scheme is lower than that for the maximum-output detection scheme. Nevertheless, the two-symbol 8PSK labels can be recognized by thresholding the outputs between 0.000785 and 0.

3. Evaluation of Noise Tolerance

To investigate the noise tolerance for the proposed waveguide-type 8PRC, we built a simulation model using OptiSytem software (Optiwave Systems Inc.). The waveguide-type QPRC

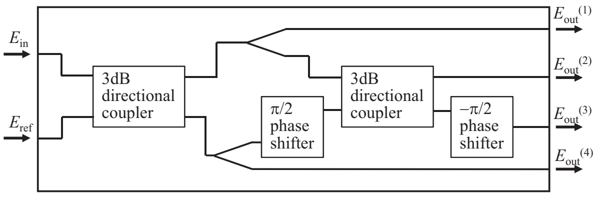

Fig. 10. A simulation model for the waveguide-type QPRC module.

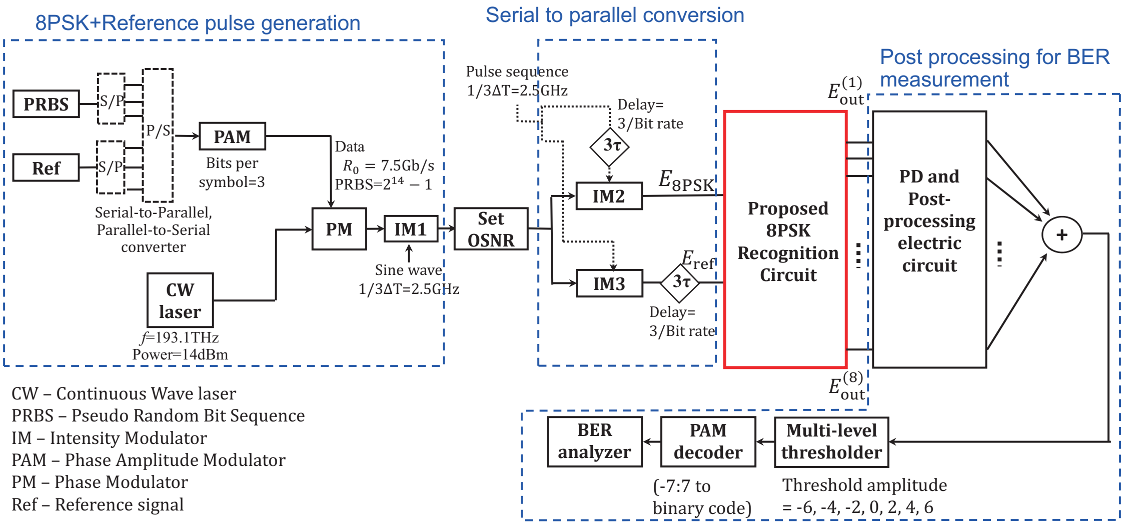

Fig. 11. A simulation setup for one-symbol 8PSK recognition circuit.

module as illustrated in Fig. 3 is modeled with discrete optical components as shown in Fig. 10. The module consists of two 3-dB directional couplers, two power dividers, a $-\pi/2$ phase shifter, and a $\pi/2$ phase shifter.

The simulation setup for one-symbol label recognition is illustrated in Fig. 11. A pseudo-random-bit sequence (PRBS) with length of $2^{14} - 1$ is used for generating nonreturn-to-zero (NRZ) sequence at a half of the bit rate R_0 for 8PSK signals. The sequence signal is connected to a serial-to-parallel (S/P) converter to make a sequence of 3-bit parallel signals. At the same time, a reference signal is generated by a user defined bit sequence generator with the same bit rate as that of the data signal and is connected to another S/P converter. A parallel-to-serial (P/S) converter is used to combine a data signal and a reference signal. The combined sequence is connected to a pulse-amplitude-modulator (PAM) to generate a modulation electric signal. To generate the optical 8PSK coded signal, we use a continuous wave (CW) laser at a frequency of 193.1 THz as a light source, a phase modulator (PM), and an intensity modulator (IM1) to carve the NRZ to the return-to-zero (RZ) pulse train.

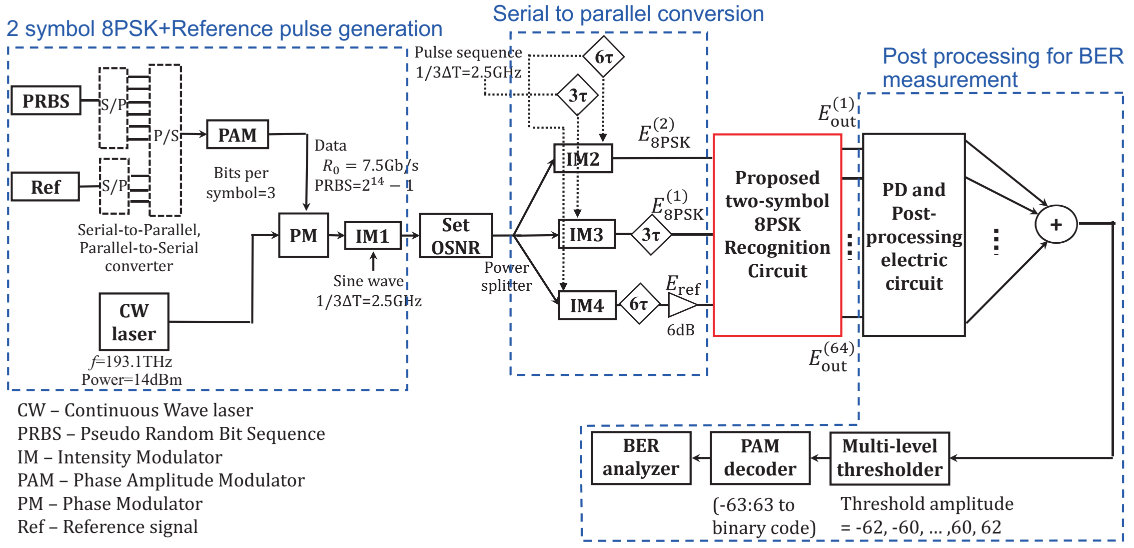

Fig. 12. A simulation setup for two-symbol 8PSK recognition circuit.

The component, named as Set OSNR, is used to add noise to the sequential train of the 8PSK pulse and the reference pulse. The noise added signals are sent to a serial to parallel conversion circuit which consists of two intensity modulators and two delay elements. The converted parallel 8PSK pulse train and the reference pulse train are incident to the proposed label recognition circuit.

Practically, optical thresholders are used to identify the maximum or minimum port after the optical recognition circuit. We employ the photodiodes (PDs) and postprocessing electric circuit instead of the optical thresholders to measure the BER to evaluate the noise tolerance in this study The circuits for the PDs and post-processing electric circuit differ in the two recognition schemes as described in the next subsections.

Figure 12 illustrates the simulation setup for two-symbol label recognition. A two-symbol 8PSK pulse sequence is combined with a sequence of the reference signal to generate the transmission pulse sequence. The received pulse sequence is converted to parallel pulse trains and sent to the proposed recognition circuit.

The constellation for typical generated 8PSK signals at OSNR of 30 dB and 20 dB is shown in Fig. 13.

3.1 Maximum-output detection scheme

The PDs and post-processing electric circuit for one-symbol 8PSK signals are shown in Fig. 14. The input signals detected by PDs are filtered by the low pass filter (LPF) with cutoff frequency of the symbol rate (= $R_0/3$), and are amplified. The amplified electric signals are

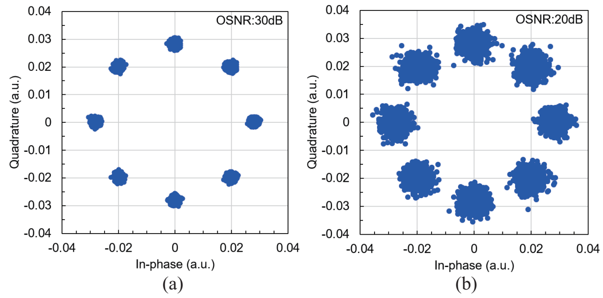

Fig. 13. Constellation for generated 8PSK signals at OSNR of (a) 30 dB and (b) 20 dB.

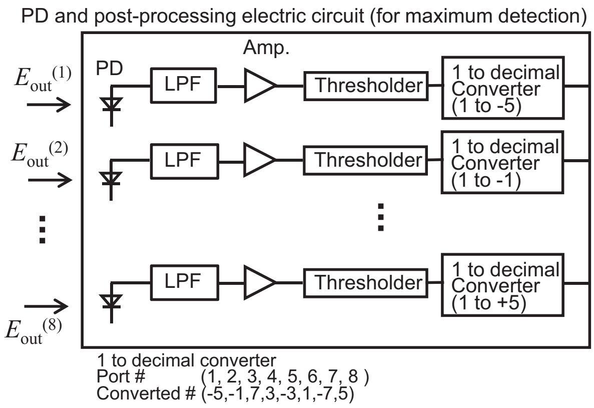

Fig. 14. The PDs and post-processing electric circuit for one-symbol 8PSK signals in the maximum-output scheme.

sent to the thresholders to extract maximum signal pulses. The amplitudes of the thresholded pulses are converted to different amplitudes by using the 1 to decimal converters to distinguish the output port of the 8PRC. Eight output signals from the postprocessing circuit are added to convert into binary codes with the PAM decoder. The output codes are compared with the incident data sequence to measure the BER by the BER analyzer. Typical signals along the recognition circuit are shown in Fig. 15, where (a) a generated combined pulse sequence for the 8PSK signal and the reference signal, (b) the phase of pulses shown in (a), (c) an output signal from the output port 1 of the 8PRC, (d) an output signal from output port 1 of the postprocessing circuit, and (e) an input signal to the final PAM decoder. The threshold level in the postprocessing circuit was set at an electrical voltage corresponding to the optical power of 0.368 mW which is in the middle of the maximum and the second maximum optical power from the 8PRC of 0.397 mW and 0.339 mW, respectively. This threshold value was chosen to optimize the BER performance.

The simulated BER performance as a function of OSNR at the receiver is shown in

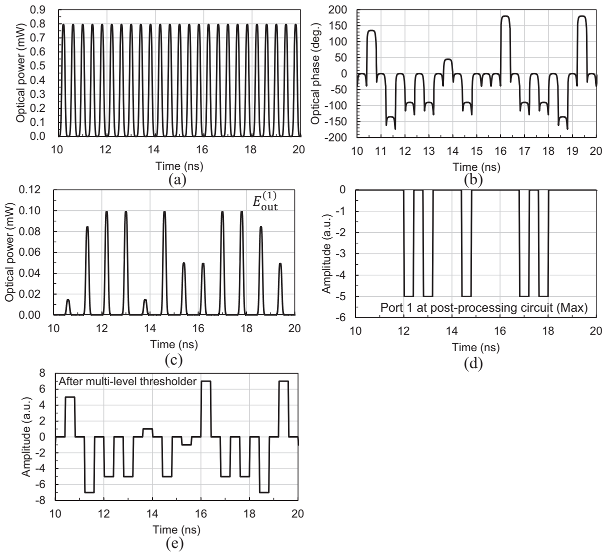

Fig. 15. Typical signals along the recognition circuit; (a) a generated combined pulse sequence for the 8PSK signal and the reference signal, (b) the phase of pulses shown in (a), (c) an output signal from the output port 1 of the 8PRC, (d) an output signal from output port 1 of the postprocessing circuit, and (e) an input signal to the final PAM decoder.

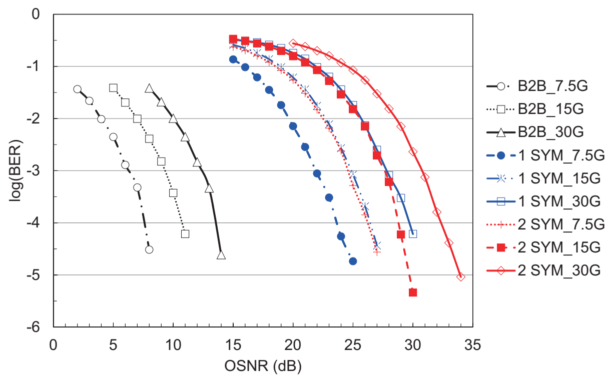

Fig. 16. BER performance for one- and two-symbol 8PSK labels by maximum output detection scheme.

Fig. 16. As a comparison, a BER measured by back-to-back (B2B) configuration is plotted by using a digital coherent receiver with adaptive equalization, frequency offset estimation, and carrier phase recovery. The BER performances at the bit rate R_0 of 7.5, 15, and 30 Gb/s are plotted. The required OSNR, for example, at BER of 1.0×10^{-3} at $R_0 = 7.5$ Gb/s is around 22 dB and 24.5 dB for 1-symbol and 2-symbol length signals, respectively. As compared with B2B BER performance, the required OSNR penalties of the proposed recognition circuit for 1-symbol and 2-symbol length signals at 7.5 Gb/s are around 15.5 dB and 18 dB, respectively. The required OSNR becomes larger by 3 dB when the bit rate is doubled.

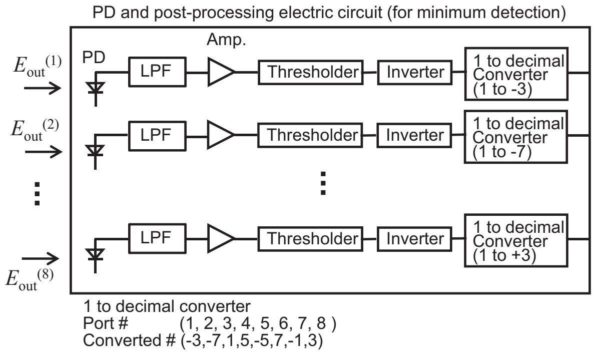

Fig. 17. The PDs and post-processing electric circuit for one-symbol 8PSK signals in the minimum-output scheme.

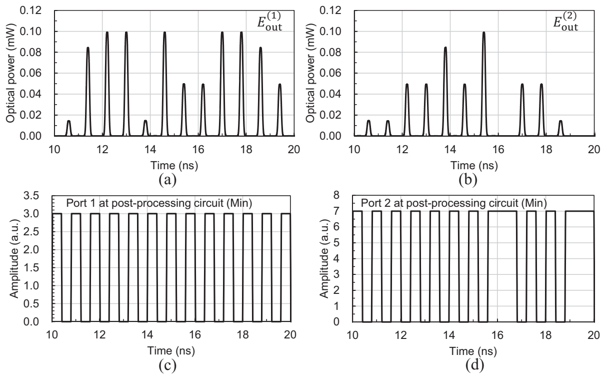

Fig. 18. Typical signals along the recognition circuit;(a) an output signal from the output port 1 of the 8PRC, (b) an output signal from the output port 12 of the 8PRC, (c) an output signal from output port 1 of the postprocessing circuit, and (d) an output signal from output port 2 of the postprocessing circuit.

3.2 Minimum-output detection scheme

The PDs and post-processing circuit for the minimum-output scheme is shown in Fig. 17. Electrical inverters are inserted in this circuit. Typical signals along the recognition circuit for the input pulse sequence as illustrated in Figs. 15(a) and (b) is shown in Fig. 18, where (a) an output signal from the output port 1 of the 8PRC, (b) an output signal from the output port 12 of the 8PRC, (c) an output signal from output port 1 of the postprocessing circuit, and (d) an output signal from output port 2 of the post-processing circuit. As seen from Figs. 18(c) and (d), repeated pulses were occurred at every two time slots corresponding to the time slots for the reference pulses. These repeated pulses cancel out by summing all the outputs from the post-processing circuit because the amplitudes of these pulses are -7, -5, -3, -1, 1, 3, 5, and 7 as shown in Fig. 17. Thus, the input signal to the final PAM decoder is the same as shown in Fig. 15(e).

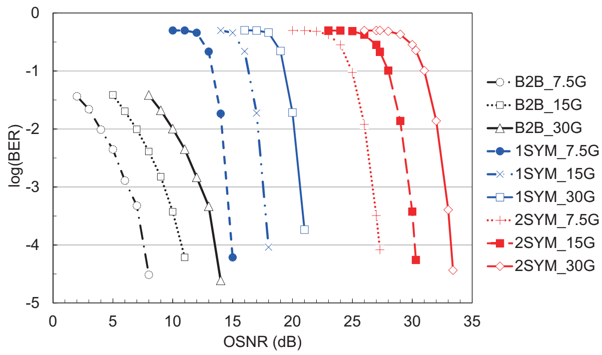

Fig. 19. BER performance for one- and two-symbol 8PSK labels by minimum output detection scheme.

The simulated BER performance as a function of OSNR at the receiver is shown in Fig. 19. The required OSNR at BER of 1.0×10^{-3} at $R_0 = 7.5$ Gb/s is around 14.5 dB and 26.8 dB for 1-symbol and 2-symbol length signals, respectively. As compared with B2B BER performance, the required OSNR penalties of the proposed circuit for 1-symbol and 2-symbol length signals at 7.5 Gb/s are around 8 dB and 18.3 dB, respectively. The required OSNR becomes larger by 3 dB when the bit rate is doubled.

Despite the better BER performance than that of the maximum-output scheme for the one-symbol signal, the performance becomes worse for the two-symbol signal. The reason for this lower scalability for the minimum-output scheme was discussed in the previous section.

4. Conclusion

We have proposed the optical waveguide-type device for recognition of optical 8PSK coded labels. The proposed device is based on the previously proposed waveguide-type circuit for recognition of QPSK coded labels. The proposed device consists of 3dB directional couplers, Y-branches, asymmetric X junction couplers, and a $-\pi/4$-phase shifter. The recognition method was theoretically discussed and the noise tolerance was also investigated. The proposed circuit could recognize from either maximum or minimum output port. These two recognition schemes were compared from the viewpoint of noise tolerance. The required OSNR at BER of 1×10^{-3} at $R_0 = 7.5$ Gb/s was around 22 dB and 14.5 dB for the maximum and minimum output schemes of one-symbol length 8PSK signals, respectively. The required OSNR becomes larger by 3 dB when the bit rate is doubled.

We also discussed the scalability for the proposed recognition circuits. The maximum-output detection scheme was found to be superior to the minimum-output one because the phase adjustment cannot be employed between the first-stage 8PRC and the second-stage 8PRCs for the minimum-output detection circuit.

References

1) A. E. Willner, S. Khaleghi, M. R. Chitgarha, M. R. Chitgarha, and O. F Yilmaz, J. Lightwave Technol., **32**(4), 660 (2013).
2) A. M. J. Koonen, N. Yan, J. J. V. Olmos, I. T. Monroy, C. Peucheret, E. V. Breusegem, and E. Zouganeli, J. of Sel. Topics in Quantum Electron., **13**(5), 1540 (2007).
3) S. J. B. Yoo, J. of Sel. Topics in Quantum Electron., **17**(2), 406 (2011).
4) K. Kitayama, N. Wada, and H. Sotobayashi, J. Lightwave Technol., **18**(12), 1834 (2000).
5) R. Clavero, J. M. Martinez, F. Ramos, and J. Marti, Opt. Express, **12**(18), 4326 (2004).
6) H. Furukawa, N. Wada, and T. Miyazaki, Optical Fiber Communication Conference (OFC2006), OWP3 (2006).
7) N. Kataoka, G. Cincotti, N. Wada, and K. Kitayama, OptoElectronics and Communication Conference (OECC2011), 8A2-5 (2011).
8) H. Brahmi, G. Giannoulis, M. Menif, V. Katopodis, D. Kalavrouziotis, C. Stamatiadis, C. Kouloumentas, H. Avramopoulos, and D. Erasme, Photon. Technol. Lett., **24**(9), 721(2012).
9) M. Xin, M. Chen, H. Chen, and S. Xie, Photon. Technol. Lett., **22**(11) 769 (2010).
10) D. J. Blumenthal, B. E. Olsson, G. Rossi, T. E Dimmick, L. Rau, M. Masanovic, O. Lavrora, R. Doshi, O. Jerphagnon, J. E. Bowers, and V. Kaman, J. Lighwave Technol., **18**(12), 2058 (2000).
11) O.Moriwaki, T. Kitoh, T. Sakamoto, and A. Okada, IEEE Photon. Technol. Lett., **17**(2), 489 (2005).
12) G. Cincotti, J. Lightwave Technol., **22**(2), 337 (2004).
13) I. Glesk, K. I. Kang, and P. R. Prucnal, Optics Express, **1**(5), 126 (1997).
14) R. Takahashi, T. Nakahara, H. Takenouchi, T. Yasui, and H. Suzuki, Optical Review, **11**(2), 98 (2004).
15) K. Sawada and H. Uenohara, J. Lightwave Technol., **28**(13) 1889 (2010).
16) S. Ibrahim, T. Nakahara, H. Ishikawa, and R. Takahashi, Opt. Express, **24**(7), 6985 (2016).
17) H. Hiura and N. Goto, IEICE Trans. Electron., **E90-C**(8), 1619 (2007).
18) H. Hiura, J. Narita, and N. Goto, IEICE Trans. Electron. **E90-C**(12), 2270 (2007).
19) Y. Makimoto, H. Hiura, N. Goto, and S. Yanagiya, J. Ligthwave Technol., **27**(1), 60 (2009).

20) T. Surenkhorol, H. Kishikawa, N. Goto, and K. Gonchigsumlaa, Optical Engineering, **56**(10), 107101 (2017).
21) K. Inoshita, H. Kishikawa, Y. Makimoto, N. Goto, and S. Yanagiya, “Proposal of optical waveguide circuits for recognition of optical QAM codes,” J. Lightwave Technol., **31**(13), 2271-2278 (2013).
22) K. Inoshita, Y. Hama, H. Kishikawa, and N. Goto, Optical Engineering, **55**(12), 126105 (2016).
23) H. Hiura, N. Goto, and S. Yanagiya, J. Lighwave Technol., **27**(24), 5543 (2009).
24) N. Odbayar, M. Adiya, H. Kishikawa, and N. Goto, CLEO Pacific Rim 2018 Conference (CLEO-pr2018), W4J.7 (2018).
25) M. Adiya, N. Odbayar, H. Kishikawa, and N. Goto, 23rd MicroOptics Conference (MOC2018), J-3 (2018).
26) H. Kishikawa, Y. Makimoto, K. Inoshita, S. Igarashi, N. Goto, and S. Yanagiya, Optical Engineering, **55**(5), 057104 (2016).
27) D. W. Stowe and T.-Y. Hsu, J. Lightwave Technol., **1**(3), 519 (1983).
28) G. A. Berenbrock and B. Schlemmer, IEEE Photon. Tech. Lett., **1**(4), 86 (1989).

I